

# Towards integrated polarization diversity: design, fabrication, and characterization of integrated polarization splitters and rotators

Michael R. Watts<sup>†</sup>, Minghao Qi<sup>†</sup>, Tymon Barwicz<sup>†</sup>, Luciano Socci<sup>‡</sup>, Peter T. Rakich<sup>†</sup>, Erich P. Ippen<sup>†</sup>, Henry I. Smith<sup>†</sup>, and Hermann A. Haus<sup>†</sup>

<sup>†</sup>Research Laboratory of Electronics, Massachusetts Institute of Technology, 77 Massachusetts Ave, Cambridge, Massachusetts 02139, USA

<sup>‡</sup>Pirelli Labs, viale Sarca, 222-20126 Milano, Italy

[mwatts@alum.mit.edu](mailto:mwatts@alum.mit.edu)

**Abstract:** Integrated mode-evolution-based polarization splitters and rotators were designed with rigorous electromagnetic simulations and fabricated with a unique multilayer fabrication strategy. Prototype devices demonstrated effective splitting and rotating of polarization with low cross-talk.

©2003 Optical Society of America

**OCIS codes:** (130.3120) Integrated optics devices; (230.5440) Polarization-sensitive devices

## 1. Introduction

High index contrast (HIC) structures typically exhibit significant polarization sensitivities. To enable polarization independent performance from HIC structures, a necessary feature for a standard single mode fiber based communications link, the polarization sensitivity may be circumvented by implementing a polarization diversity scheme [1,2]. Such an approach requires the arbitrary polarization emanating from a fiber to be split into orthogonal components. By further rotating one of the outputs, a single polarization may be realized on-chip and the two paths may be operated on in parallel with identical structures. An integrated approach allows for the devices to be batch fabricated and the path lengths of the two arms to be matched through lithography.

Integrated mode-evolution-based polarization splitters and rotators have recently been reported on [8-10]. In contrast to structures based on mode-coupling [2-5], these structures were shown through three-dimensional finite-difference time-domain (FDTD) simulations to exhibit little wavelength dependence. Moreover, mode-evolution-based devices [6,7] are typically fabrication tolerant. The structures mate directly to one another to form an integrated polarization splitter-rotator (PSR). Adopting a unique multilayer fabrication strategy, structures similar to those reported in [9,10] were fabricated. Results of standalone and integrated polarization splitters and rotators will

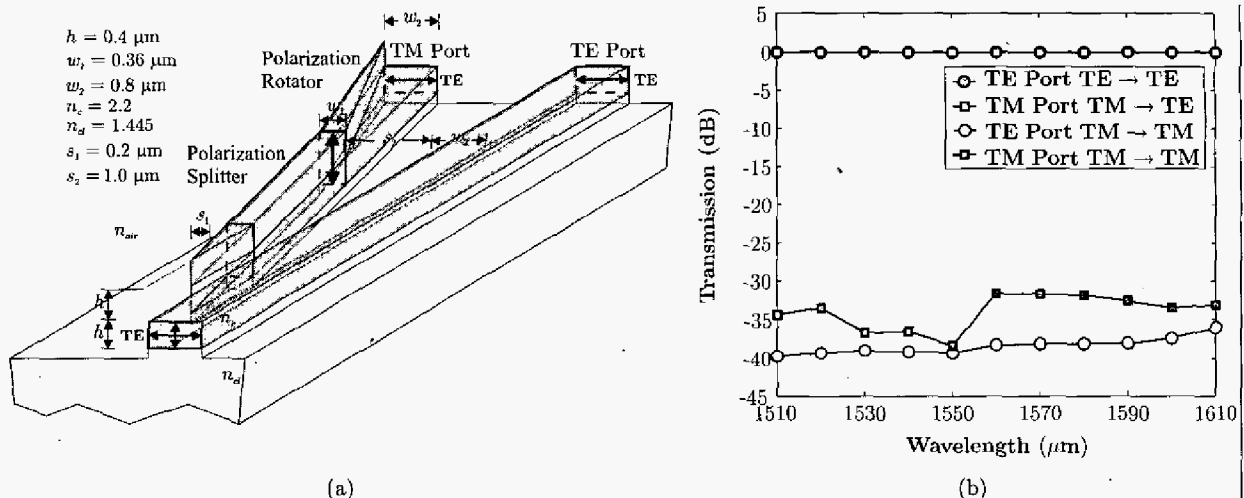


Fig. 1. (a) Integrated mode evolution based polarization splitter-rotator and (b) EME results for an 800.6  $\mu\text{m}$  long device. be presented and compared to FDTD [11] and eigenmode expansion (EME) [12] results.

## 2. Polarization splitter and rotator design

The polarization splitter and rotator designs are based largely on those described in [9] and [10] except here no upper cladding is used. The combined polarization splitter-rotator structure, depicted in Fig. 1a, is formed from two silicon nitride core layers ( $n_c = 2.2$ ), an under-cladding of thermal oxide ( $n_{cl} = 1.445$ ) and an over-cladding of air.

The operating principle of both the polarization splitter and rotator devices is mode-evolution. With mode-evolution-based devices it is important to suppress mode-coupling introduced by the evolution of the structure. To minimize power exchange between modes, a slow evolution of the structure is needed to allow the modes a chance to de-phase before substantial power exchange occurs. In [9,10] EME was shown to agree with three-dimensional FDTD for these types of devices. In Fig. 1b EME simulations of an integrated polarization splitter and rotator are presented. In the simulated structure, the rotator length was chosen to be  $384\ \mu\text{m}$  and the polarization splitter length to be  $416.6\ \mu\text{m}$ . The waveguide dimensions are as depicted in Fig. 1a. The simulations demonstrate broadband that low cross-talk performance is possible with this type of structure.

### 3. Fabrication and experimental results

The PSR in Fig. 1a is a two-layer structure and generally requires a planarization step to allow the deposition of the second material layer. We note that the pattern in the second layer is a subset of that in the first layer, and the two layers are made from the same type of material. A novel “one deposition and two-step etching” process can be applied to avoid the planarization step (Fig. 2a~2e)). First,  $820\text{nm}$  of silicon nitride (SiN,  $n = 2.2$ ) was deposited via low-temperature chemical vapor deposition (Fig. 2a). Second, two hard masks were created with electron-beam

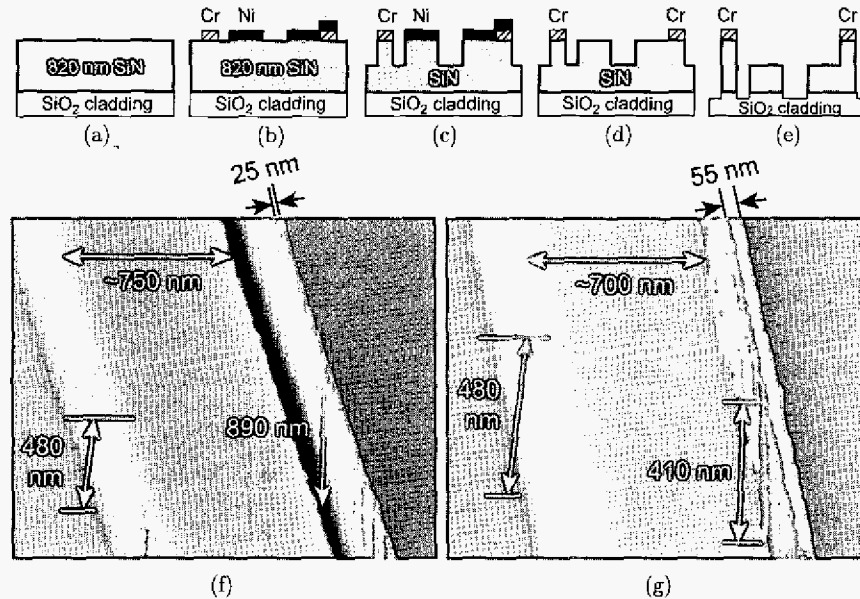


Fig. 2. (a)~(e): Fabrication process for the PSR. SEM images of a (f) polarization splitter input and (g) polarization rotator output.

lithography and lift-off (Fig. 2b). The first hard mask was  $50\text{-nm}$  thick chromium (Cr), defining the pattern of tall waveguides. The second one,  $50\text{-nm}$  thick nickel (Ni), defined the short waveguides and was properly aligned to the first one. Third, the waveguide patterns were transferred into SiN via reactive-ion-etching, using a mixture of  $\text{CHF}_3$  and  $\text{O}_2$ . The etching was divided into two steps to properly define waveguides of different heights. The first etch stopped when  $410\text{ nm}$  of SiN was removed (Fig. 2c). One type of the hard masks, namely Ni, was selectively removed (Fig. 2d) and the second etch removed the remaining  $410\text{nm}$  of SiN, as well as an additional  $70\text{ nm}$  of  $\text{SiO}_2$  underneath, to ensure that SiN was completely etched through. The short waveguides, without the protection of hard masks, preserved the height and cross-sections while their vertical location was recessed  $410\text{ nm}$  as a result of the second-step etch. The tall waveguides, protected by Cr, had a full height of  $820\text{ nm}$ . The fourth and final step was the removal of Cr via wet-etch (Fig. 2e). The fabricated structures are shown in Fig. 2f and 2g with minimum feature sizes down to  $25\text{ nm}$ .

Both  $192\ \mu\text{m}$  and  $384\ \mu\text{m}$  long rotators were fabricated along with  $208.3\ \mu\text{m}$  and  $416.6\ \mu\text{m}$  long polarization splitters. Both standalone and integrated devices were made. For all devices, both  $360\text{ nm}$  and  $378\text{ nm}$  wide tall waveguides were fabricated. This was primarily an effort to avoid phase-matched TM modes in the polarization splitter. Also, because the tolerance on the hard mask alignment was not clear, aligned and  $\pm 50\text{ nm}$  misalignments of the hard masks were used on all devices. The transmission spectra for polarization splitters, rotators and integrated splitters and rotators were measured using a tunable laser across the  $1.51\text{-}1.61\ \mu\text{m}$  band. Despite the

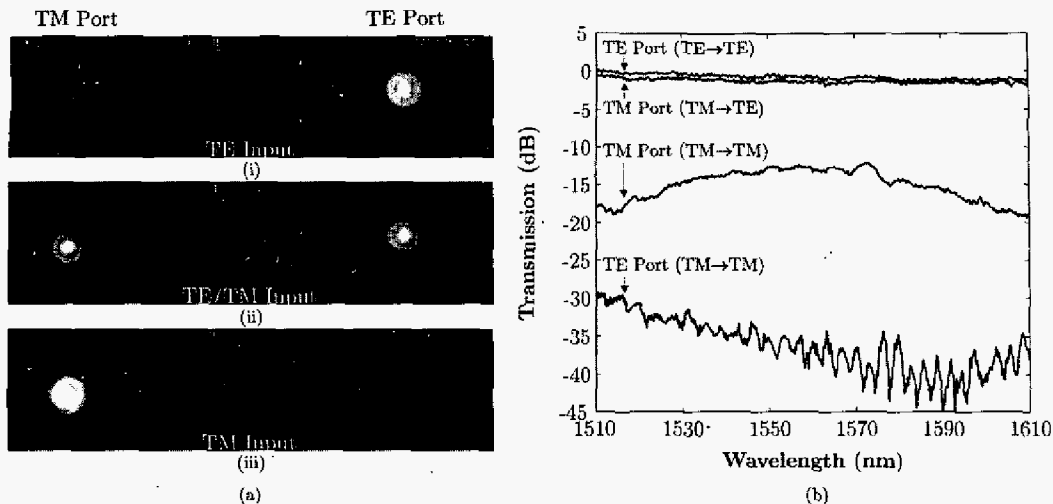


Fig. 3. (a) Infrared image of PSR output for (i) TE, (ii) TE/TM, and (iii) TM inputs, and (b) Measured performance across 1510 – 1610 nm. Note: The TM port should (and does) possess a TE polarization as a result of the polarization rotator.

intentional width variations and misalignments of the layers, nearly all of the fabricated devices, splitters, rotators and integrated splitters and rotators demonstrated broadband low cross-talk performance. The performance of a representative integrated polarization splitter and rotator is depicted in Fig. 3a and Fig. 3b. The results in Fig. 3b were normalized to the respective straight waveguide losses and chip couplings. The performance of the integrated polarization splitter and rotator qualitatively matches the simulation results. The structure exhibits broadband low cross-talk performance. The cross-talk level is below -30 dB in the TE port and -11 dB in the TM port across the measured spectrum. Other PSRs exhibited more impressive performance, but had noncontiguous waveguides resulting from e-beam stage drift making it difficult to normalize out the data. The best standalone polarization rotator exhibited less -18 dB cross-talk across the band while the best polarization splitter exhibited -20 dB cross-talk across the 1.51-1.61 $\mu$ m band. As a result of noncontiguous waveguides and imperfect chip facets it is difficult to ascertain the losses. However, the device losses do not appear to be significant.

#### 4. Conclusions

For the first time to our knowledge an integrated polarization splitter and rotator has been demonstrated. The structure was designed using rigorous electromagnetic simulations and fabricated in silicon nitride using a unique multilayer fabrication strategy. The devices were characterized and the integrated polarization splitter and rotator was shown to exhibit cross-talk levels below -30 dB for the TE port and -11 dB for the TM port. In addition, the best standalone polarization splitters and rotators exhibited less than -20 dB and -18 dB cross-talk, respectively. Importantly, these devices open up the possibility of achieving chip-level polarization independence with densely integrated high index contrast polarization dependent devices.

#### References

- [1] C. K. Madsen, "Optical all-pass filters for polarization mode dispersion compensation," *Optics Letters* **25**, 878-880, (2000).
- [2] M. R. Watts, "Wavelength switching and routing through evanescently induced absorption," MS Thesis, (Department of Electrical Engineering and Computer Science, Massachusetts Institute of Technology, Cambridge, MA, 2001).
- [3] J. J. G. M. van der Tol and J. H. Laarhuis, "A short polarization splitter without metal overlays on InGaAsP-InP," *J. Lightwave Tech.* **9**, 879 (1991).
- [4] J. Z. Huang, R. Scarmozzino, G. Nagy, M. J. Steel, and R. M. Osgood, "Realization of a compact and single-mode optical passive polarization converter," *IEEE Photon. Technol. Lett.* **12**, 317-319, (2000).
- [5] V. P. Tzolov and M. Fontaine, "A passive polarization converter free of longitudinally periodic structure," *Optics Communications* **127**, 7-13, (1996).
- [6] Y. Shani, C. H. Henry, R. C. Kistler, R. F. Kazarinov and K. J. Orlowsky, "Integrated optic adiabatic polarization splitter on silicon," *Appl. Phys. Lett.* **56**, 120-121 (1990).
- [7] R. M. de Ridder, A. F. M. Sander, A. Driessen, J. H. J. Fluitman, "An integrated optic adiabatic TE/TM mode splitter on silicon," *J. Lightwave Technol.* **11**, 1806-1811 (1993).
- [8] M.R. Watts, H.A. Haus, G. Gorni, and M. Cherchi, "Polarization splitting and rotating through adiabatic transitions," *Proceedings of Integrated Photonics Research Conference 2003 (IPR 2003)*, 26-28 (2003).
- [9] M. R. Watts and H. A. Haus, "Integrated mode-evolution-based polarization rotators," *Optics Letters*, **30**, 138-140 (2005).
- [10] M. R. Watts, H. A. Haus, and E. P. Ippen, "An integrated mode-evolution-based polarization splitter," *Optics Letters*, to be published.
- [11] A. Taflov, *Computational Electrodynamics: The Finite-Difference Time-Domain Method* (Norwood, MA: Artech House, 1995)
- [12] FIMMWAVE by Photon Design®